Reversible Decomposition of Secondary Phases in BaO Infiltrated LSM Electrodes-Polarization Effects

Traulsen, Marie Lund; McIntyre, Melissa D.; Norrman, Kion; Sanna, Simone; Mogensen, Mogens Bjerg; Walker, Robert A.

Published in:
Advanced Materials Interfaces

Link to article, DOI:
10.1002/admi.201600750

Publication date:
2016

Document Version
Peer reviewed version

Supporting Information

Reversible Decomposition of Secondary Phases in BaO Infiltrated LSM Electrodes – Polarization Effects

Marie L. Traulsen, Melissa D. McIntyre, Kion Norrman, Simone Sanna, Mogens B. Mogensen and Robert A. Walker*

E-mail: matr@dtu.dk

SI-1 XRD recorded on porous LSM-CGO composite electrodes infiltrated with BaO

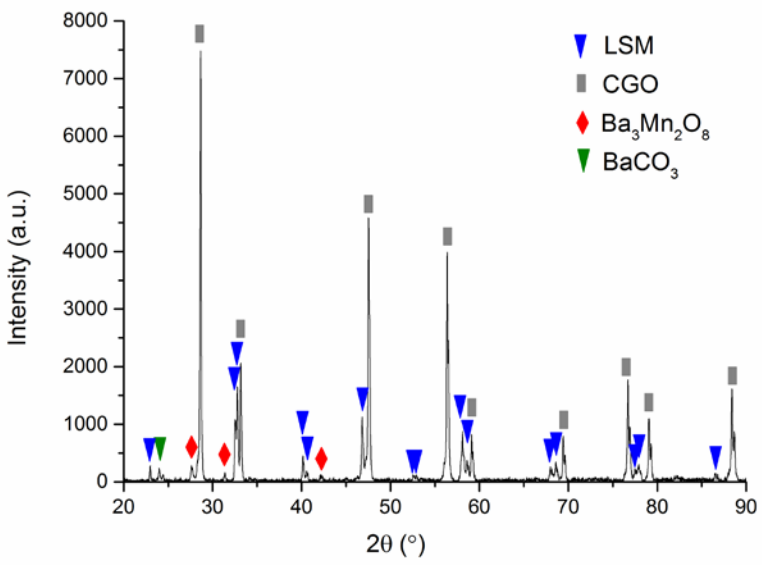

Figure S1. XRD recorded on porous LSM-CGO composite electrodes infiltrated with BaO prior to Raman spectroscopy experiments.

SI-2 Synthesis and characterization of $Ba_3Mn_2O_8$

One material that was relatively poorly characterized by Raman spectroscopy was $Ba_3Mn_2O_8$. Consequently, $Ba_3Mn_2O_8$ was synthesized according to the procedure described by Weller *et al.*[1] for subsequent Raman characterization. First, stoichiometric amounts of $BaCO_3$ (Sigma-Aldrich) and Mn_2O_3 (Sigma-Aldrich) were mixed in ethanol for 6 h on a ball-mill. The

mixture was then dried, transferred to a crucible and heated to 900 °C under flowing air for 24 h. The sample was air-quenched from 900 °C directly to room temperature. XRD measurements after the synthesis showed a nearly pure phase of $Ba_3Mn_2O_8$ with only very minor phase impurities from $BaMnO_3$ and $BaCO_3$ (Figure S3-a).

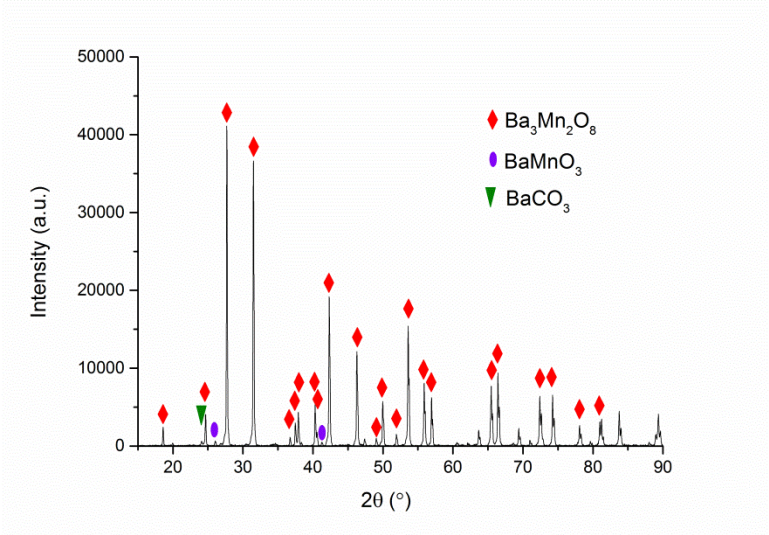

Figure S2-a. XRD recorded on synthesized $Ba_3Mn_2O_8$.

A representative Raman spectrum recorded from the synthesized $Ba_3Mn_2O_8$ is shown in Figure S3-b and contains two dominant peaks at 301 cm^{-1} and 771 cm^{-1}. The presence of these peaks, along with the results from the XRD data, indicates that $Ba_3Mn_2O_8$ formed on the BaO infiltrated LSM electrodes. Furthermore, the Raman spectrum of $Ba_3Mn_3O_8$ is similar to the Raman spectra of $Sr_3V_2O_8$ and $Ba_3V_2O_8$ reported in literature[2]. Based on these studies the 301 cm^{-1} vibrational band can be ascribed to O-Mn-O bending while the 717 cm^{-1} and 771 cm^{-1} bands are assigned to Mn-O stretching.

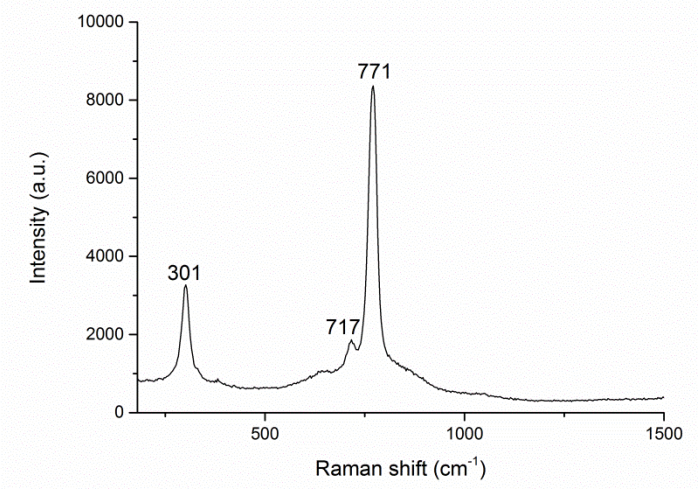

Figure S2-b. Raman spectrum recorded on synthesized $Ba_3Mn_2O_8$.

SI-3 Reproducibility between porous composite electrodes and model thin film electrodes

LSM thin film electrodes served as model electrodes to investigate how the addition of BaO affects the electrocatalytic properties for O_2 reduction on LSM electrodes. To verify that the chemical species observed on these model electrodes were also present on porous electrodes used in typical applications, additional experiments were performed on LSM-CGO composite electrodes both with and without BaO. *In situ* Raman spectra collected on the plain and BaO infiltrated LSM-CGO porous composite electrodes are shown in Figure S2. A spectrum recorded on the BaO containing LSM thin film is included for comparison. The vibrational modes at approximately 306 cm^{-1} and 773 cm^{-1} are distinct for both BaO infiltrated samples and are assigned to $Ba_3Mn_2O_8$ while the 1051 cm^{-1} peak is assigned to either MnO[3] or $BaCO_3$ [4] . The strong peak at 450 cm^{-1} corresponds to CGO and is shifted to lower frequencies relative to the commonly reported 462 cm^{-1} due to the elevated operational temperature[5]. Minor peaks observed at 610 cm^{-1} and 662 cm^{-1} are assigned to MnO_2 [6-8] and Mn_2O_3 [6]respectively. A weak feature at 202 cm^{-1} was observed on the porous composite LSM electrode and is attributed to the lattice vibrations in the LSM[9].

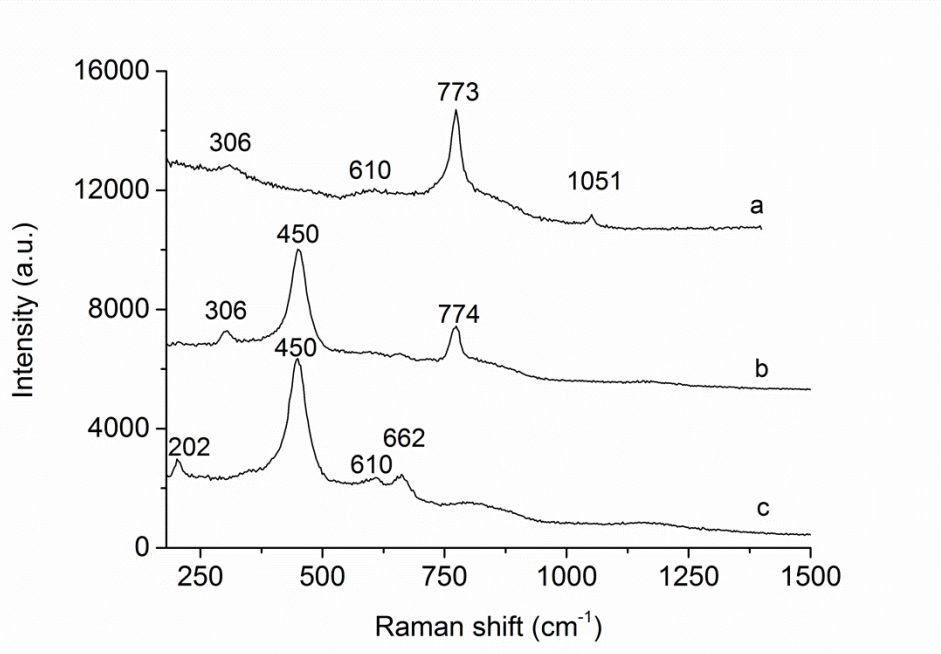

Figure S3. Representative Raman spectra recorded at 500 °C in 10% O_2 flow on a) the LSM thin film electrode with BaO, b) the porous LSM-CGO electrode infiltrated with BaO and c) the porous LSM-CGO composite electrode without infiltration. The spectra are shifted on the Y-axis and re-scaled to facilitate comparisons.

SI-4 Representative chronoamperomentry curve

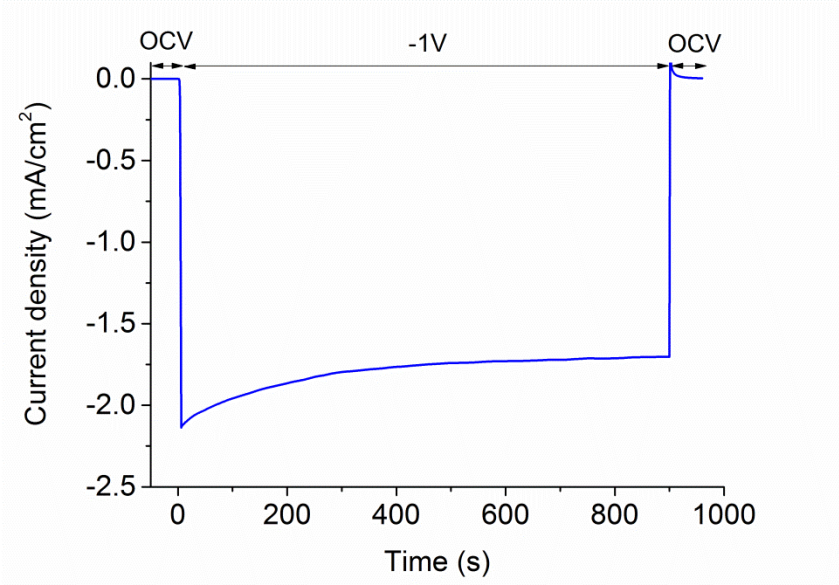

Figure S4. Representative chronoamperometry curve for BaO infiltrated LSM thin film electrode at 500 °C in 10% O_2 with Ar polarized at -1 V.

SI-5: Raman spectra at 300 °C

Relative peak intensities within a given spectrum showed consistent and reproducible quantitative differences as a function of temperature. For example, the feature at 690 cm^{-1} is more pronounced in Raman spectra recorded at 300°C compared to spectra recorded at 500 °C. These differences are likely due to reduced line broadening and the better signal-to-noise ratios at the lower temperature.

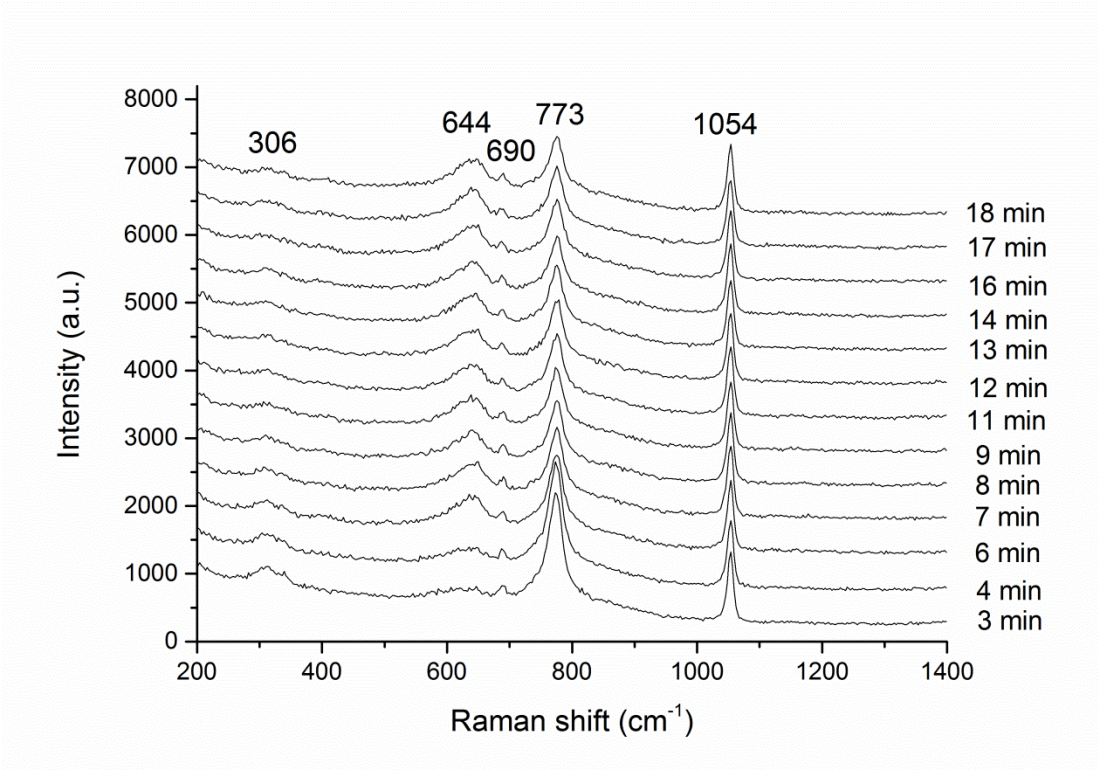

Figure S5-a. Raman spectra recorded on LSM thin film electrode with BaO deposition at 300 °C in 10% O_2 before and during the onset of -1V applied potential.

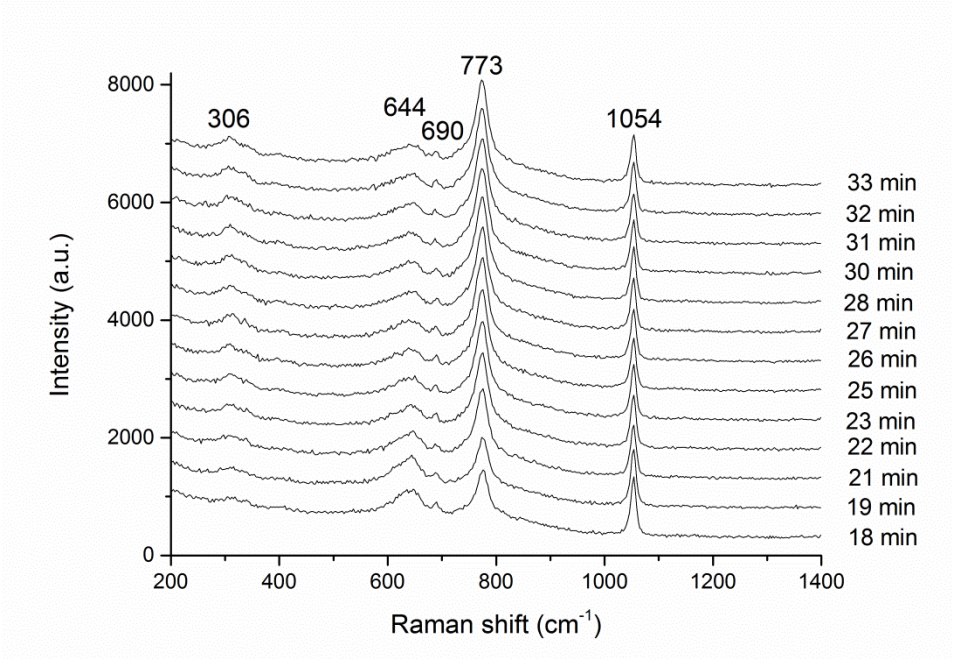

Figure S5-b Raman spectra recorded on LSM thin film electrode with BaO deposition at 300 °C in 10% O_2 before and during a +1 V potential was applied to the cell. The bottom spectrum was recorded with the cell polarized at -1 V prior to switching the applied potential to +1 V.

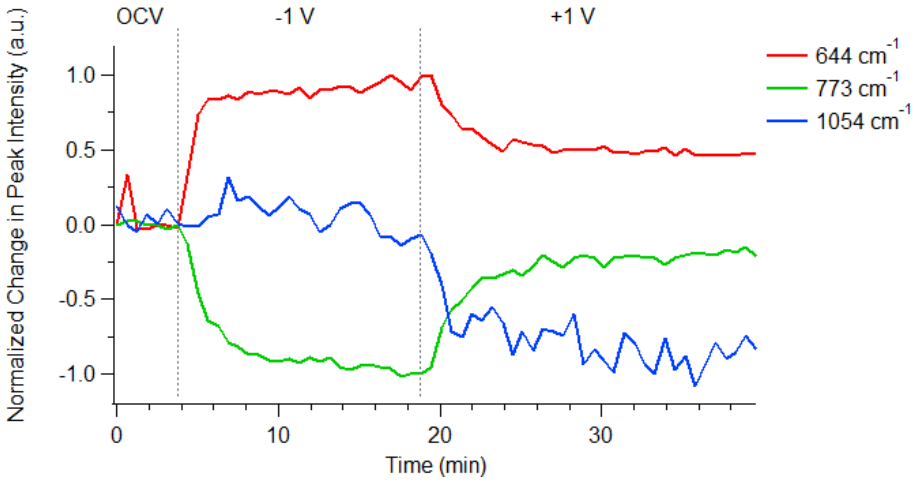

Figure S5-c Normalized change in peak intensity from Raman spectra collected on a BaO infiltrated LSM thin film electrode at 300 °C with 10% O_2 during -1V polarization followed immediately by +1V polarization.

SI-6 Normalized peak intensity plot at 500 °C

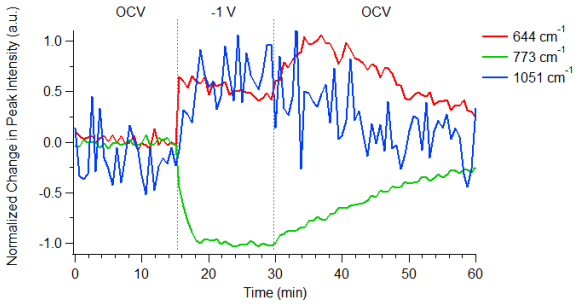

Figure S6. Normalized change in peak intensity from Raman spectra collected on a BaO infiltrated LSM thin film electrode at 500 °C with 10% O_2 prior to, during and after -1V polarization. During this experiment the 644 cm^{-1} peak increased more rapidly than the 773 cm^{-1} peak increased immediately after applying the -1 V polarisation.

SI-7 SEM image of thin film electrode

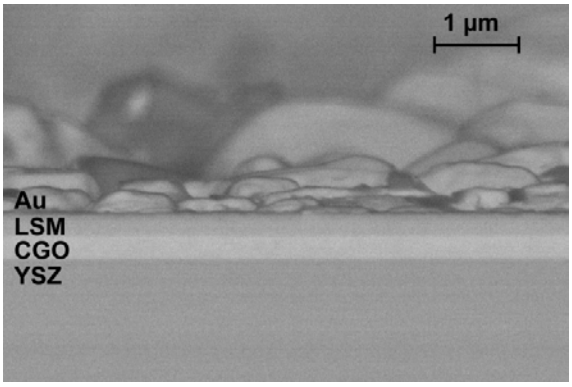

Figure S7. SEM image of broken cross-section of an electrochemical thin film model cell, showing (from top to bottom) the sputtered Au layer, LSM thin film, CGO thin film and YSZ electrolyte.

References in the SI

[1] M. T. Weller, S. J. Skinner, *Acta Crystallogr. , Sect. C: Cryst. Struct. Commun.* **1999**, *55*, 154.

[2] A. Grzechnik, P. F. McMillan, *J. Solid State Chem.* **1997**, *132*, 156.

[3] N. Mironova-Ulmane, A. Kuzmin, M. Grube, *J. Alloys Compounds.* **2009**, *480*, 97.

[4] W. Kaabar, S. Bott, R. Devonshire, *Spectrochim. Acta Mol. Biomol. Spectrosc.* **2011**, *78*, 136.

[5] R. C. Maher, L. F. Cohen, *J. Phys. Chem. A.* **2008**, *112*, 1497.

[6] F. Buciuman, F. Patcas, R. Craciun, D. Zahn, *Phys. Chem. Chem. Phys.* **1999**, *1*, 185.

[7] T. Gao, H. Fjellvag, P. Norby, *Anal. Chim. Acta.* **2009**, *648*, 235.

[8] B. Banov, A. Momchilov, M. Massot, C. M. Julien, *Mater. Sci. Eng. , B.* **2003**, *100*, 87.

[9] V. B. Podobedov, A. Weber, D. B. Romero, J. P. Rice, H. D. Drew, *Solid State Commun.* **1998**, *105*, 589.